
Intra Order-Preserving Functions for Calibration of Multi-Class Neural Networks

Amir Rahimi^{1*} Amirreza Shaban^{2*} Ching-An Cheng^{3*} Byron Boots⁴ Richard Hartley¹

Abstract

Predicting calibrated confidence scores for multi-class deep networks is important for avoiding rare but costly mistakes. A common approach is to learn a post-hoc calibration function that transforms the output of the original network into calibrated confidence scores while maintaining the network’s accuracy. However, previous post-hoc calibration techniques work only with simple calibration functions, potentially lacking sufficient representation to calibrate the complex function landscape of deep networks. In this work, we aim to learn general post-hoc calibration functions that can preserve the top- k predictions of any deep network. We call this family of functions *intra order-preserving* functions. We propose a new neural network architecture that represents a class of intra order-preserving functions by combining common neural network components. Additionally, we introduce order-invariant and diagonal sub-families, which can act as regularization for better generalization when the training data size is small. We show the effectiveness of the proposed method across a wide range of datasets and classifiers. Our method outperforms state-of-the-art post-hoc calibration methods, namely temperature scaling and Dirichlet calibration, in multiple settings.

as default components in building decision systems; for example, a multi-class neural network can be treated as a probabilistic predictor and its softmax output can provide the confidence scores of different actions for the downstream decision making pipeline (Girshick, 2015; Cao et al., 2017; Mozafari et al., 2019). While this is an intuitive idea, recent research has found that deep networks, despite being accurate, can be overconfident in their predictions, exhibiting high calibration error (Maddox et al., 2019; Guo et al., 2017; Kendall & Gal, 2017). In other words, trusting the network’s output naively as confidence scores in system design could cause undesired consequences: a serious issue for applications where mistakes are costly, such as medical diagnosis and autonomous driving.

A promising approach to address the miscalibration is to augment a given network with a parameterized calibration function (e.g. learnable layers). This extra component is tuned post-hoc using a held-out calibration dataset, so that the effective full network becomes calibrated (Guo et al., 2017; Kull et al., 2019; 2017b;a; Platt et al., 1999; Zadrozny & Elkan, 2001). In contrast to usual deep learning, the calibration dataset here is typically *small*. Therefore, learned calibration functions can easily overfit and actually reduce the accuracy of the given network (Guo et al., 2017; Kull et al., 2019). A careful design regularization and parameterization of calibration functions is imperative.

The calibration function is often inserted between the last few layers of the given network as a form of regularization. A classical non-parametric technique is isotonic regression (Zadrozny & Elkan, 2002), which learns a staircase calibration function and is guaranteed to preserve the accuracy. But the complexity of non-parametric learning can be too expensive to provide the needed generalization (Kull et al., 2017b;a). By contrast, Guo et al. (2017) proposed to simply learn a scalar parameter to rescale the original output logits, at the cost of being suboptimal in calibration (Maddox et al., 2019); see also Section 6. Recently, Kull et al. (2019) proposed Dirichlet calibration to learn linear transformations of the output logits. While this scheme is more flexible than the temperature scaling above, it fails to guarantee accuracy preservation.

However, none of the existing approaches is ideal, because

1. Introduction

Deep neural networks have demonstrated impressive accuracy in classification tasks, such as image recognition (He et al., 2016; Ren et al., 2015) and medical research (Jiang et al., 2012; Caruana et al., 2015). These exciting results have recently motivated engineers to adopt deep networks

¹Australian National University, Australian Center for Robotic Vision ²Georgia Tech ³Microsoft Research ⁴Washington University.

* Equal Contribution

. Correspondence to: Amir Rahimi <amir.rahimi@anu.edu.au>.

Work under review.

they compromise either the accuracy (Kull et al., 2019) or the flexibility (Platt et al., 1999; Guo et al., 2017) of the calibrated network. Limiting the expressivity of calibration functions can be an issue, especially when calibrating deep networks with complicated functional landscapes. A preferable hypothesis space needs to be expressive and, at the same time, provably preserve the accuracy of any given network it calibrates.

In this paper, we introduce a new family of functions, called *intra order-preserving* functions, which precisely describes this ideal hypothesis space. Informally speaking, an intra order-preserving function $\mathbf{f} : \mathbb{R}^n \rightarrow \mathbb{R}^n$ is a vector-valued function whose output values always share the same ordering as the input values across the n dimensions. For example, if $\mathbf{x} \in \mathbb{R}^n$ is increasing from coordinate 1 to n , then so is $\mathbf{f}(\mathbf{x})$. Because of this property, a post-hoc calibration function keeps the top- k class prediction, *if and only if* it is an intra order-preserving function.

This formal definition allows us to systematically study network calibration. We identify necessary and sufficient conditions for describing intra order-preserving functions, and propose a novel neural network architecture that can represent complex intra order-preserving function through common neural network components. In addition, we introduce order-invariant and diagonal structures, which can act as regularization to improve generalization.

Learning the post-hoc calibration function within the intra order-preserving family therefore presents a solution to the dilemma where previous approaches compromise accuracy or flexibility. We conduct several experiments to validate the benefits of learning with these new functions in post-hoc network calibration. The results demonstrate improvement over various calibration performance metrics, compared with the original network, temperature scaling (Guo et al., 2017), and Dirichlet calibration (Kull et al., 2019).

2. Problem Setup

We address the problem of calibrating neural networks for n -class classification. Define $[n] := \{1, \dots, n\}$. Let $\mathcal{Z} \subseteq \mathbb{R}^d$ be the domain, $\mathcal{Y} = [n]$ be the label space, and let Δ_n denote the $n - 1$ dimensional unit simplex. Suppose we are given a trained probabilistic predictor $\phi_o : \mathbb{R}^d \rightarrow \Delta_n$ and a small calibration dataset \mathcal{D}_c of i.i.d. samples drawn from an unknown distribution π on $\mathcal{Z} \times \mathcal{Y}$. For simplicity of exposition, we assume that ϕ_o can be expressed as the composition $\phi_o =: \mathbf{sm} \circ \mathbf{g}$, with $\mathbf{g} : \mathbb{R}^d \rightarrow \mathbb{R}^n$ being a non-probabilistic n -way classifier and $\mathbf{sm} : \mathbb{R}^n \rightarrow \Delta_n$ being the softmax operator¹, i.e.

$$\mathbf{sm}_i(\mathbf{x}) = \frac{\exp(\mathbf{x}_i)}{\sum_{j=1}^n \exp(\mathbf{x}_j)}, \quad \text{for } i \in \mathcal{Y}, \quad (1)$$

where the subscript i denotes the i th element of a vector. When queried at $\mathbf{z} \in \mathcal{Z}$, the probabilistic predictor ϕ_o returns $\arg \max_i \phi_{o,i}(\mathbf{z})$ as the predicted label and $\max_i \phi_{o,i}(\mathbf{z})$ as the associated confidence score. (The top- k prediction is defined similarly.) We say $\mathbf{g}(\mathbf{z})$ is the *logits* of \mathbf{z} with respect to ϕ_o .

Given ϕ_o and \mathcal{D}_c , our goal is to learn a post-hoc calibration function $\mathbf{f} : \mathbb{R}^n \rightarrow \mathbb{R}^n$ such that the new probabilistic predictor $\phi := \mathbf{sm} \circ \mathbf{f} \circ \mathbf{g}$ is better calibrated *and* keeps the accuracy (or similar performance concepts like top- k accuracy) of the original network ϕ_o . That is, we want to learn new logits $\mathbf{f}(\mathbf{g}(\mathbf{z}))$ of \mathbf{z} . As we will discuss, this task is non-trivial, because while learning \mathbf{f} might improve calibration, doing so could also risk over-fitting to the small dataset \mathcal{D}_c and damaging accuracy. To make this statement more precise, below we first review the definition of calibration and then discuss challenges in learning \mathbf{f} with \mathcal{D}_c .

2.1. Calibration Metrics

We first review the definition of perfect calibration (Guo et al., 2017) and common calibration metrics.

Definition 1. For a distribution π on $\mathcal{Z} \times \mathcal{Y}$ and a probabilistic predictor $\psi : \mathbb{R}^d \rightarrow \Delta_n$, let random variables $\mathbf{z} \in \mathcal{Z}$, $y \in \mathcal{Y}$ be distributed according to π , and define random variables $\hat{y} := \arg \max_i \psi_i(\mathbf{z})$ and $\hat{p} := \psi_{\hat{y}}(\mathbf{z})$. We say ψ is *perfectly calibrated* with respect to π , if for any $p \in [0, 1]$,

$$\text{Prob}(\hat{y} = y | \hat{p} = p) = p \quad (2)$$

Note that \mathbf{z} , y , \hat{y} and \hat{p} are correlated random variables. Therefore, the definition in (2) essentially means that, if ψ is perfectly calibrated, then, for any $p \in [0, 1]$, the true label y and the predicted label \hat{y} matches, with a probability exactly p in the events where \mathbf{z} satisfies $\max_i \psi_i(\mathbf{z}) = p$.

We remark that Definition 1 depends not only on the conditional distribution $\pi(y|\mathbf{z})$, but also on the marginal distribution $\pi(\mathbf{z})$. As a result, perfect calibration is an orthogonal concept to accuracy. For example, for any π on $\mathcal{Z} \times \mathcal{Y}$, there is a perfectly calibrated probabilistic predictor that always outputs a constant class distribution (i.e. it always predicts the same label regardless of the input); however, this predictor has very poor accuracy.

In practice, learning a perfectly calibrated predictor is unrealistic, so we need a way to measure the calibration error. A common calibration metric is called Expected Calibration Error (ECE) (Naeini et al., 2015): $\text{ECE} = \sum_{m=1}^M \frac{|B_m|}{N} |\text{acc}(B_m) - \text{conf}(B_m)|$. This equation is calculated in two steps: First the confidence scores of samples in \mathcal{D}_c are partitioned into M equally spaced bins $\{B_m\}_{m=1}^M$.

¹The softmax requirement is not an assumption but for making the notation consistent with the literature. The proposed algorithm can also be applied to the output of general probabilistic predictors.

Second the weighted average of the differences between the average confidence $\text{conf}(B_m) = \frac{1}{|B_m|} \sum_{i \in B_m} \hat{p}^i$ and the accuracy $\text{acc}(B_m) = \frac{1}{|B_m|} \sum_{i \in B_m} \mathbb{1}(y^i = \hat{y}^i)$ in each bin is computed as the ECE metric, where $|B_m|$ denotes the size of bin B_m , $\mathbb{1}$ is the indicator function, and the superscript i indexes the sampled random variable.

In addition to ECE, other calibration metrics have also been proposed (Guo et al., 2017; Nixon et al., 2019; Brier, 1950). For example, Maximum Calibration Error (MCE) (Guo et al., 2017), which similarly to ECE partitions the confidence scores into equally spaced bins, measures instead the maximal difference of average confidence and accuracy over all bins. Brier score (Brier, 1950; Kull et al., 2019), on the other hand, computes the mean squared difference between confidence scores and one-hot encoded ground-truth labels.

While the calibration metrics above measure the deviation from perfect calibration in (2), they are usually not suitable loss functions for optimizing neural networks, e.g., due to the lack of continuity or non-trivial computation time. Instead, the calibration function \mathbf{f} in $\phi = \mathbf{sm} \circ \mathbf{f} \circ \mathbf{g}$ is often optimized indirectly through a surrogate loss function (e.g. the negative log-likelihood) defined on the held-out calibration dataset \mathcal{D}_c (Guo et al., 2017; Kull et al., 2019).

2.2. Importance of Regularization

Unlike regular deep learning scenarios, here the calibration dataset \mathcal{D}_c is relatively small. Therefore, controlling the capacity of the hypothesis space of \mathbf{f} becomes a crucial topic. There is typically a trade-off between preserving accuracy and improving calibration: Learning \mathbf{f} could improve the calibration performance, but it could also change the decision boundary of ϕ from ϕ_o decreasing the accuracy. Most recent work sacrifices calibration performance to maintain the accuracy, as we rely on the new predictor ϕ for classification at the test time. While using simple calibration functions may be applicable when ϕ_o has a simple function landscape or is already close to being well calibrated, such a function class might not be sufficient to calibrate modern deep networks with complex decision boundaries.

The observation above motivates us to investigate the possibility of learning calibration functions within a hypothesis space that can provably guarantee preserving the accuracy of the original network ϕ_o . The identification of such functions would resolve the previous dilemma and allow us to study precisely the needed structure to ensure generalization of calibration when the calibration dataset \mathcal{D}_c is small.

3. Intra Order-Preserving Functions

In this section, we formally describe this desirable class of functions for post-hoc network calibration. We name them *intra order-preserving functions*. We will show that learn-

ing within this family is both necessary and sufficient to keep the top- k accuracy of the original network unchanged. We also study additional function structures on this family (e.g. limiting how different dimensions can interact), which can be used as regularization in learning calibration functions. Last we discuss a new neural network architecture for representing these functions.

3.1. Setup: Sorting and Ranking

We begin by defining sorting functions and ranking. Let $\mathbb{P}^n \subset \{0, 1\}^{n \times n}$ denote the set of $n \times n$ permutation matrices. We say a vector $\mathbf{t} \in \mathbb{R}^n$ is a *tie breaker* if $\mathbf{t} = \mathbf{P}\mathbf{r}$, for some $\mathbf{P} \in \mathbb{P}^n$, where $\mathbf{r} = [1, \dots, n]^\top \in \mathbb{R}^n$. We will use tie breakers to resolve ties in ranking as described below.

Suppose some tie breaker \mathbf{t} is selected beforehand, which will be used throughout the analyses and computation. Given a vector $\mathbf{x} \in \mathbb{R}^n$, we say $S : \mathbb{R}^n \rightarrow \mathbb{P}$ is a *sorting function* if $\mathbf{y} = S(\mathbf{x})\mathbf{x}$ satisfies $\mathbf{y}_1 \geq \mathbf{y}_2 \geq \dots \geq \mathbf{y}_n$, where S breaks ties according to the ordering given in the tie breaker \mathbf{t} , satisfying $S(\mathbf{e})\mathbf{r} = \mathbf{t}$, where \mathbf{e} is the vector of ones. We say two vectors $\mathbf{u}, \mathbf{v} \in \mathbb{R}^n$ share the same *ranking* if $S(\mathbf{u}) = S(\mathbf{v})$ for *any* tie breaker \mathbf{t} .

3.2. Intra Order-Preserving Functions

We now define the *intra* order-preserving property with respect to different coordinates of a single vector input.

Definition 2. We say a function $\mathbf{f} : \mathbb{R}^n \rightarrow \mathbb{R}^n$ is *intra order-preserving*, if, for any $\mathbf{x} \in \mathbb{R}^n$, \mathbf{x} and $\mathbf{f}(\mathbf{x})$ share the same ranking.

The output of an intra order-preserving function $\mathbf{f}(\mathbf{x})$ maintains *all* ties and strict inequalities between elements of the input vector \mathbf{x} . Namely, for all $i, j \in [n]$, we have $\mathbf{x}_i > \mathbf{x}_j$ (or $\mathbf{x}_i = \mathbf{x}_j$) if and only if $\mathbf{f}_i(\mathbf{x}) > \mathbf{f}_j(\mathbf{x})$ (or $\mathbf{f}_i(\mathbf{x}) = \mathbf{f}_j(\mathbf{x})$). For example, a simple intra order-preserving function is the positive scaling $\mathbf{f}(\mathbf{x}) = \mathbf{x}/t$ for some $t > 0$. Another common instance is the softmax operator defined in (1).

Applying an intra order-preserving function as the calibration function in $\phi = \mathbf{sm} \circ \mathbf{f} \circ \mathbf{g}$ does not change top- k predictions between ϕ and $\phi_o = \mathbf{sm} \circ \mathbf{g}$. This can be seen as follows: Let $\mathbf{x} = \mathbf{g}(\mathbf{z})$ be the logits with respect to ϕ_o . Given any tie breaker, one can use the sorting function S to extract the top- k indices of \mathbf{x} through $S(\mathbf{x})\mathbf{x}$. Since $S(\mathbf{f}(\mathbf{x})) = S(\mathbf{x})$ when \mathbf{f} is intra order-preserving, the top- k indices remain the same for ϕ and ϕ_o .

Next, we provide a necessary and sufficient condition for constructing continuous, intra order-invariant functions. This theorem will be later used to design neural network architectures for learning calibration functions.

Theorem 1. A continuous function $\mathbf{f} : \mathbb{R}^n \rightarrow \mathbb{R}^n$ is *intra order-preserving*, if and only if $\mathbf{f}(\mathbf{x}) = S(\mathbf{x})^{-1} \mathbf{U} \mathbf{w}(\mathbf{x})$ with \mathbf{U} being an upper-triangular matrix of ones and $\mathbf{w} : \mathbb{R}^n \rightarrow$

\mathbb{R}^n being a continuous function such that

- $\mathbf{w}_i(\mathbf{x}) = 0$, if $\mathbf{y}_i = \mathbf{y}_{i+1}$ and $i < n$,
- $\mathbf{w}_i(\mathbf{x}) > 0$, if $\mathbf{y}_i > \mathbf{y}_{i+1}$ and $i < n$,
- $\mathbf{w}_n(\mathbf{x})$ is arbitrary,

where $\mathbf{y} = S(\mathbf{x})\mathbf{x}$ is the sorted version of \mathbf{x} .

The proof is deferred to Appendix. Here we provide as sketch as to why Theorem 1 is true. Since $\mathbf{w}_i(\mathbf{x}) \geq 0$ for $i < n$, applying the matrix U on $\mathbf{w}(\mathbf{x})$ results in a sorted vector $U\mathbf{w}(\mathbf{x})$ (which is the cumulative sum of $\mathbf{w}(\mathbf{x})$). Thus, applying $S(\mathbf{x})^{-1}$ further on $U\mathbf{w}(\mathbf{x})$ makes sure that $\mathbf{f}(\mathbf{x})$ has the same ordering as the input vector \mathbf{x} . The reverse direction can be proved similarly. For the continuity, observe that the sorting function $S(\mathbf{x})$ is piece-wise constant and only changes values, when there is a tie appears or disappears in the input \mathbf{x} . This means that if the corresponding elements in $U\mathbf{w}(\mathbf{x})$ are also equally valued when a tie happens, the discontinuity of the sorting function S does not affect the continuity of \mathbf{f} inherited from \mathbf{w} .

3.3. Order Invariant and Diagonal Sub-families

Here we discuss two additional structures interesting to intra order-preserving functions: *order-invariant* and *diagonal* properties. When these structures are applicable, the learning of calibration functions can generalize better. Similar to the purpose of the previous section, we will study necessary and sufficient conditions of intra order-preserving functions with these properties.

First, we study the concept of order invariant functions.

Definition 3. We say a function $\mathbf{f} : \mathbb{R}^n \rightarrow \mathbb{R}^n$ is *order-invariant*, if $\mathbf{f}(P\mathbf{x}) = P\mathbf{f}(\mathbf{x})$ for all $\mathbf{x} \in \mathbb{R}^n$ and $P \in \mathbb{P}^n$.

For an order-invariant function \mathbf{f} , when two elements \mathbf{x}_i and \mathbf{x}_j in the input \mathbf{x} are swapped, the corresponding elements $\mathbf{f}_i(\mathbf{x})$ and $\mathbf{f}_j(\mathbf{x})$ in the output $\mathbf{f}(\mathbf{x})$ also swap. Thus, if we restrict learning calibration functions within order invariant functions, the mapping learned for the i th class can also be used for the j class. This property becomes helpful, when the calibration dataset \mathcal{D}_c is insufficient to learning the calibration functions for all of the classes independently.

We characterize in the theorem below the properties of functions that are both intra order-preserving and order-invariant (an instance of these functions is the softmax operator in (1)). That is, to make an intra order-preserving function also order-invariant, we just need to feed the function \mathbf{w} in Theorem 1 instead with the sorted input $\mathbf{y} = S(\mathbf{x})\mathbf{x}$. This scheme makes the learning of \mathbf{w} easier since it always receives sorted vectors.

Theorem 2. A continuous, intra order-preserving function $\mathbf{f} : \mathbb{R}^n \rightarrow \mathbb{R}^n$ is order invariant, if and only if $\mathbf{f}(\mathbf{x}) = S(\mathbf{x})^{-1}U\mathbf{w}(\mathbf{y})$, where U , \mathbf{w} , and \mathbf{y} are in Theorem 1.

Another structure of interest here is the diagonal property.

Definition 4. We say a function $\mathbf{f} : \mathbb{R}^n \rightarrow \mathbb{R}^n$ is *diagonal*, if $\mathbf{f}(\mathbf{x}) = [\mathbf{f}_1(\mathbf{x}_1), \dots, \mathbf{f}_n(\mathbf{x}_n)]$ for $f_i : \mathbb{R} \rightarrow \mathbb{R}$ with $i \in [n]$.

In the context of calibration, a diagonal calibration function means that different class predictions do not interact with each other in $\phi = \mathbf{sm} \circ \mathbf{f} \circ \mathbf{g}$.

The next theorem relates diagonal intra order-preserving functions to increasing functions.

Theorem 3. A continuous, intra order-preserving function $\mathbf{f} : \mathbb{R}^n \rightarrow \mathbb{R}^n$ is diagonal, if and only if $\mathbf{f}(\mathbf{x}) = [\bar{f}(\mathbf{x}_1), \dots, \bar{f}(\mathbf{x}_n)]$ for some continuous and increasing function $\bar{f} : \mathbb{R} \rightarrow \mathbb{R}$.

Compared with general diagonal functions, diagonal intra order-preserving automatically implies that the same function \bar{f} is shared across all dimensions. Thus, learning with diagonal intra order-preserving functions benefits from parameter-sharing across different dimensions, which could drastically decrease the number of parameters.

Furthermore, functions in this sub-family are automatically order invariant and inter order-preserving.

Definition 5. We say a function $\mathbf{f} : \mathbb{R}^m \rightarrow \mathbb{R}^n$ is *inter order-preserving* if, for any $\mathbf{x}, \mathbf{y} \in \mathbb{R}^m$ such that $\mathbf{x} \geq \mathbf{y}$, $\mathbf{f}(\mathbf{x}) \geq \mathbf{f}(\mathbf{y})$, where \geq denotes elementwise comparison.

Corollary 1. A diagonal, intra order-preserving function is order invariant and inter order-preserving

Note that inter and intra order-preserving are orthogonal definitions. Inter order-preserving is also an important property for calibration functions, since this property guarantees that $\mathbf{f}_i(\mathbf{x})$ increases with the original class logit \mathbf{x}_i .

Finally, it is worth mentioning that the temperature scaling scheme (Guo et al., 2017) uses a strict subset (i.e. $\bar{f}(\mathbf{x}_i) = \mathbf{x}_i/t$ for some $t > 0$) of the diagonal intra order-preserving functions. Therefore, although diagonal intra order-preserving functions may sound limiting in learning calibration functions, they still represent a family larger than the common temperature scaling scheme.

Fig. 1 summarizes the relationship between different order-preserving functions.

3.4. Practical Considerations

Theorem 1 and Theorem 2 describe general representations of intra order-preserving functions through using the function \mathbf{w} that satisfies certain non-negative constraints. Here we propose a neural network architecture for parameterizing \mathbf{w} , which automatically meets these constraints and makes learning calibration functions an unconstrained optimization problem. The idea is to break \mathbf{w} into smaller functions. For $i < n$, we set $\mathbf{w}_i(\mathbf{x}) = \sigma(\mathbf{y}_i - \mathbf{y}_{i+1})\mathbf{m}_i(\mathbf{x})$, where

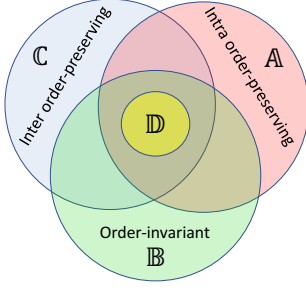


Figure 1. Relationship between different function families. Theorem 1 specifies the intra order-preserving functions \mathbb{A} . Theorem 2 specifies the intra order-preserving and order-invariant functions $\mathbb{A} \cap \mathbb{B}$. Theorem 3 specifies the diagonal intra order-preserving functions \mathbb{D} . By Corollary 1, these functions are also order-invariant and inter order-preserving i.e. $\mathbb{D} \subseteq \mathbb{A} \cap \mathbb{B} \cap \mathbb{C}$.

$\sigma : \mathbb{R} \rightarrow \mathbb{R}$ is a positive function that is zero only when $x = 0$, and \mathbf{m}_i is a strictly positive function.

It is easy to verify that the proposed architecture satisfies the requirements on \mathbf{w} . However, we note that this class of functions cannot represent all possible \mathbf{w} stated in Theorem 1. In general, the rate $\mathbf{w}_i(\mathbf{x}) \rightarrow 0$ can be a function of \mathbf{x} , but in the proposed factorization above, the rate of convergence to zero is controlled by σ , which is a function of solely two elements y_i and y_{i+1} .

Fortunately, such a limitation does not substantially decrease the expressiveness of \mathbf{f} in practice, because the subspace where \mathbf{w}_i vanishes has zero measure in \mathbb{R}^n (i.e. subspaces where there is at least one tie in $\mathbf{x} \in \mathbb{R}^n$).

By Theorem 1 and Theorem 2, the proposed architecture ensures $\mathbf{f}(\mathbf{x})$ is continuous in \mathbf{x} as long as $\sigma(y_i - y_{i+1})$ and $\mathbf{m}_i(\mathbf{x})$ are continuous in \mathbf{x} . In Appendix, we show that this is true when σ and \mathbf{m}_i are continuous functions. Additionally, we prove that when σ and \mathbf{m} are differentiable and $\frac{d\sigma(a)}{da}$ has a zero at $a = 0$, $\mathbf{f}(\mathbf{x})$ is also differentiable with respect to \mathbf{x} .

4. Implementation

Given a calibration dataset $\mathcal{D}_c = \{(\mathbf{z}^i, y^i)\}_{i=1}^N$ and a calibration function \mathbf{f} parameterized by some vector $\boldsymbol{\theta}$, we define the empirical calibration loss as

$$\text{loss} = \frac{1}{N} \sum_{i=1}^N \ell(y^i, \mathbf{f}(\mathbf{x}^i)) + \frac{\lambda}{2} \|\boldsymbol{\theta}\|^2 \quad (3)$$

where $\mathbf{x}^i = \mathbf{g}(\mathbf{z}^i)$, $\ell : \mathcal{Y} \times \mathbb{R}^n \rightarrow \mathbb{R}$ is a classification cost function, and $\lambda \geq 0$ is the regularization weight. Here we follow the calibration literature (Thulasidasan et al., 2019; Guo et al., 2017; Kull et al., 2019) and use the negative log likelihood (NLL) loss in (3), i.e. $\ell(y, \mathbf{f}(\mathbf{x})) = -\log(\text{sm}_y(\mathbf{f}(\mathbf{x})))$, where sm is the softmax operator in Eq. (1). We use the NLL loss in all the experiments to study

the benefit of learning \mathbf{f} with different structures within the intra order-preserving family. The study of other loss functions for calibration (Seo et al., 2019; Xing et al., 2020) is outside the scope of this paper.

To ensure \mathbf{f} is within the intra order-preserving family, we restrict \mathbf{f} to have the structure in Theorem 1 and set $\mathbf{w}_i(\mathbf{x}) = \sigma(y_i - y_{i+1})\mathbf{m}(\mathbf{x})$, as described in Section 3.4. We parameterize function \mathbf{m} by a generic multi-layer neural network and utilize the softplus activation $s^+(a) = \log(1 + \exp(a))$ on the last layer when strict positivity is desired. We employ the Huber function (Huber, 1992)

$$L_\delta(a) = \begin{cases} \frac{a^2}{2}, & |a| < \delta \\ \delta(|a| - \frac{\delta}{2}), & \text{otherwise} \end{cases}$$

to represent σ . The Huber function satisfies all the requirements on the derivative of σ discussed above, and therefore parameterizing \mathbf{f} in this way ensures that $\mathbf{f}(\mathbf{x})$ is differentiable with respect to \mathbf{x} . In addition, because the Huber function behaves as positive scaling, when the input to σ is away from zero, we can think of \mathbf{m} as learning to scale the gaps between consecutive values in \mathbf{y} . For example, when $\mathbf{m}_i(\mathbf{x})$ is constant, our architecture recovers the temperature scaling scheme (Guo et al., 2017) almost surely.

The order-invariant version in Theorem 2 can be constructed similarly. The only difference is that the neural network that parameterizes \mathbf{m} receives instead the sorted input. Fig. 2 illustrates the architecture of these models.

The diagonal intra order-preserving version in Theorem 3 is formed by learning an increasing function shared across all logit dimensions. We follow the implementation of (Wehenkel & Louppe, 2019), which we briefly describe here. The main idea is to learn an increasing function $\bar{f}(x) : \mathbb{R} \rightarrow \mathbb{R}$ using a generic neural network. This can be realized by learning instead a strictly positive function $\bar{f}'(x)$ and a bias $\bar{f}(0) \in \mathbb{R}$. Then the desired function \bar{f} can be recovered by the integral $\bar{f}(x) = \int_0^x \bar{f}'(t)dt + \bar{f}(0)$. In implementation, the derivative \bar{f}' is modeled by a generic neural network and the positiveness is enforced by using a proper activation function in the last layer. In the forward computation, the integral is approximated numerically using Clenshaw-Curtis quadrature (Clenshaw & Curtis, 1960) and the backward pass is performed by utilizing Leibniz integral rule to reduce memory footprint. We use the official implementation of the algorithm provided by (Wehenkel & Louppe, 2019).

5. Related Work

Many different post-hoc calibration methods have been studied in the literature (Platt et al., 1999; Guo et al., 2017; Kull et al., 2019; 2017b;a). Their main difference is in the parametric family of the calibration function. In Platt scaling (Platt et al., 1999), scale and shift parameters $a, b \in \mathbb{R}$

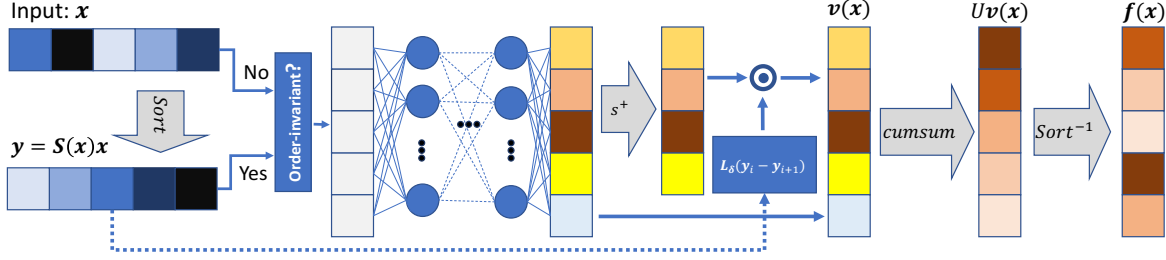


Figure 2. Flow graph of the intra order-preserving function. The vector $\mathbf{x} \in \mathbb{R}^n$ is the input to graph. The gap scale function \mathbf{m} is estimated using a generic multi-layer neural network with non-linear activation for the hidden layers. The input to the network is sorted for learning order-preserving functions. We employ softplus activation function s^+ to impose strict positivity constraints. Note that, for efficiency purposes, we use cumulative sum operation to compute $U\mathbf{v}(\mathbf{x})$.

are used to transform the scalar logit output $x \in \mathbb{R}$ i.e. $f(x) = ax + b$ of a binary classifier. Temperature scaling (Guo et al., 2017) is a simple extension of Platt scaling for multi-class calibration in which only a single scalar temperature parameter is learned. Dirichlet calibration (Kull et al., 2019) allows learning within a richer linear functions family $f(\mathbf{x}) = W\mathbf{x} + \mathbf{b}$, where $W \in \mathbb{R}^{n \times n}$ and $\mathbf{b} \in \mathbb{R}^n$ but the learned calibration function may also change the decision boundary of the original model; Kull et al. (2019) suggested regularizing the off-diagonal elements of W to avoid overfitting. Earlier works like isotonic regression (Zadrozny & Elkan, 2002), histogram binning (Zadrozny & Elkan, 2001), and Bayesian binning (Zadrozny & Elkan, 2002) are also post-hoc calibration methods.

In contrast to post-hoc calibration methods, several researches proposed to modify the training process to learn a calibrated network in the first place. Data augmentation methods (Thulasidasan et al., 2019; Yun et al., 2019) overcome overfitting by enriching the training data with new artificially generated pseudo data points and labels. Mixup (Zhang et al., 2018) creates pseudo data points by computing the convex combination of randomly sampled pairs. Cutmix (Yun et al., 2019) uses a more efficient combination algorithm specifically designed for image classification in which two images are combined by overlaying a randomly cropped part of the first image on the second image. In label smoothing (Pereyra et al., 2017; Müller et al., 2019), the training loss is augmented to penalize high confidence outputs. To discourage overconfident predictions, (Seo et al., 2019) modifies the original NLL loss by adding a cross-entropy loss term with respect to the uniform distribution. Similarly, (Kumar et al., 2018) adds a calibration regularization to the NLL loss via kernel mean embedding.

Bayesian neural networks (Gal & Ghahramani, 2016; Maddox et al., 2019) derive the uncertainty of the prediction by making stochastic perturbations of the original model. Notably, (Gal & Ghahramani, 2016) uses dropout as approximate Bayesian inference. (Maddox et al., 2019) estimates

the posterior distribution over the parameters and uses samples from this distribution for Bayesian model averaging. These methods are computationally inefficient since they typically feed each sample to the network multiple times.

6. Experiments

We evaluate the performance of intra order-preserving (OP), order-invariant intra order-preserving (OI), and diagonal intra order-preserving (DIAGONAL) families in calibrating the output of various image classification deep networks and compare their results with the previous post-hoc calibration techniques. The source code will be available under acceptance.

Datasets. We employ four different datasets: CIFAR-10, CIFAR-100 (Krizhevsky et al., 2009), SVHN (Netzer et al., 2011), and ImageNet (Deng et al., 2009). In these datasets, the number of classes vary from 10 to 1000. We evaluate the performance of different methods in calibrating three deep networks: ResNet (He et al., 2016), Wide ResNet (Zagoruyko & Komodakis, 2016), and DenseNet (Huang et al., 2017). We use the pre-computed logits of these networks provided by (Kull et al., 2019). The size of the calibration and the test datasets, as well as the number of classes for each dataset, are shown in Table 1.

Hyperparameters and Architecture Selection. We follow the experiment protocol in (Kull et al., 2019) and use cross validation on the calibration dataset to find the best hyperparameters and architectures for all the methods. We limit our architecture to fully connected networks and vary the number of hidden layers as well as the size of each layer. We allow networks with up to 3 hidden layers in all the experiments. In CIFAR-10, SVHN, and CIFAR-100 with fewer classes, we test networks with $\{1, 2, 5, 10, 20, 50, 100\}$

Dataset	#classes	Calibration dataset size	Test dataset size
CIFAR-10	10	5000	10000
SVHN	10	6000	26032
CIFAR-100	100	5000	10000
ImageNet	1000	25000	25000

Table 1. Statistics of the Evaluation Datasets.

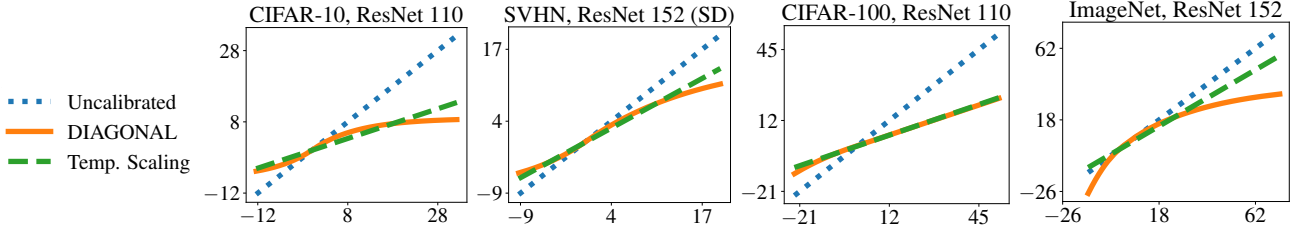


Figure 3. Transformation learned by DIAGONAL function compared to temperature scaling and uncalibrated model (identity map).

Dataset	Model	Uncalibrated	Temp. Scaling	Dir-ODIR	MS-ODIR	DIAGONAL	OI	OP
CIFAR10	ResNet 110	0.04750 ₇ (93.56%)	0.01053 ₄	0.01086 ₆ (−0.05%)	0.01059 ₅ (−0.05%)	0.00754 ₂	0.00583 ₁	0.00990 ₃
CIFAR100	ResNet 110	0.18480 ₇ (71.48%)	0.02424 ₄	0.02822 ₆ (+0.16%)	0.02735 ₅ (+0.07%)	0.02291 ₃	0.01264 ₁	0.01639 ₂
CIFAR10	Wide ResNet 32	0.04505 ₇ (93.93%)	0.00804 ₄	0.00837 ₅ (+0.31%)	0.00727 ₃ (+0.26%)	0.00692 ₂	0.00685 ₁	0.01116 ₆
CIFAR100	Wide ResNet 32	0.18784 ₇ (73.82%)	0.01480 ₂	0.01891 ₄ (+0.11%)	0.02581 ₆ (+0.12%)	0.01477 ₁	0.01480 ₂	0.02205 ₅
CIFAR10	DenseNet 40	0.05500 ₇ (92.42%)	0.00937 ₂	0.01097 ₄ (+0.05%)	0.00988 ₃ (+0.08%)	0.00916 ₁	0.01312 ₅	0.01567 ₆
CIFAR100	DenseNet 40	0.21156 ₇ (70.00%)	0.00928 ₂	0.01138 ₃ (+0.13%)	0.02197 ₅ (+0.39%)	0.00908 ₁	0.01311 ₄	0.03188 ₆
SVHN	ResNet 152 (SD)	0.00862 ₇ (98.15%)	0.00597 ₂	0.00582 ₁ (+0.04%)	0.00604 ₃ (−0.00%)	0.00608 ₄	0.00697 ₅	0.00825 ₆
Avg. Rank		7.00	2.86	4.14	4.29	2.00	2.71	4.86

 Table 2. ECE (with $M = 15$ bins) on various image classification datasets and models with different calibration methods. The subscript numbers represent the rank of the corresponding method on the given model/dataset. The accuracy of the uncalibrated model is shown in parentheses. The number in parentheses in Dir-ODIR and MS-ODIR methods show the relative change in accuracy for each method.

units per layer and for the larger ImageNet dataset, we allow a wider range of $\{5, 10, 20, 50, 100, 500\}$ units per layer. We use the similar number of units for all the hidden layers to reduce the search space. We utilize L-BFGS (Liu & Nocedal, 1989) for temperature scaling and diagonal intra order-preserving (DIAGONAL) methods on CIFAR and SVHN datasets and use Adam (Kingma & Ba, 2014) optimizer for other experiments.

Baselines. We compare the proposed function structures with temperature scaling (Guo et al., 2017), Dirichlet calibration with off-diagonal regularization (Dir-ODIR) (Kull et al., 2019), and matrix scaling with off-diagonal regularization (MS-ODIR) (Kull et al., 2019) as they are the current best performing post-hoc calibration methods. We also present the results of the original uncalibrated models for comparison. As we are using the same logits as (Kull et al., 2019), we report their results directly on CIFAR-10, CIFAR-100, and SVHN. However, since they do not present the results for ImageNet dataset, we report the results of their official implementation² on this dataset.

6.1. Results on CIFAR and SVHN Datasets

Table 2 illustrates the results of our calibration methods compared with the baselines in terms of ECE ($M = 15$ bins). OI (order-invariant and intra order-preserving family) is the superior method in ResNet 110 models and its ECE is about half of the other baselines. Its performance is similar to the other baselines in Wide ResNet, though slightly worse on SVHN dataset.

²https://github.com/dirichletcal/experiments_dnn/

Temperature scaling and DIAGONAL outperform other methods in DenseNet 40 which shows the importance of diagonal structure in these experiments. On the other hand, DIAGONAL outperforms temperature scaling in most of the cases, because DIAGONAL can learn more flexible functions (as is illustrated in Fig. 3). Note that learning intra order-preserving functions without order-invariant and diagonal assumptions (i.e OP) does not exhibit a good performance. This result highlights being simply intra order-preserving can still be too general, and extra proper regularization on this family needs to be imposed.

Overall, our DIAGONAL has the best average ranking followed by OI among the models and datasets presented in Table 2. Fig. 3 illustrates the difference between the mappings learned by DIAGONAL and temperature scaling. DIAGONAL is capable of learning complex increasing functions while temperature scaling only scales all the logits. Compared with Dir-ODIR and MS-ODIR which learn a linear transformation, all intra order-preserving methods can learn more complex transformations on the logits while maintaining the top- k accuracy of the original models. Although Dir-ODIR and MS-ODIR were able to maintain the accuracy of the original models on these datasets (Kull et al., 2019), there is no guarantee that a linear transformation maintains the accuracy in general. This specially becomes harder when the number of classes grows as we will explore in the ImageNet experiment.

6.2. Large-Scale Results on ImageNet Dataset

We report the results of post-hoc calibration methods on various metrics on the large-scale ImageNet dataset with

Intra Order-preserving Functions for Calibration of Multi-Class Neural Networks

Method	Top-1(%)	Top-5(%)	ECE	MCE	Brier	NLL	Classwise ECE	Architecture
Uncalibrated	76.20	93.04	0.06543	0.14291	0.000338	0.98848	0.32692	N/A
Temp. Scaling	76.20	93.04	0.02055	0.06840	0.000332	0.94207	0.31474	(1, 1)
Dir-ODIR	75.38	92.88	0.04795	0.09856	0.000345	0.983306	0.33017	(1000, 1000)
MS-ODIR	75.39	92.90	0.04038	0.07675	0.000343	0.97384	0.32664	(1000, 1000)
DIAGONAL	76.20	93.04	0.01027	0.11448	0.000329	0.92531	0.32059	(1, 10, 10, 1)
OI	76.20	93.04	0.01661	0.04717	0.000331	0.93531	0.31729	(1000, 100, 100, 1000)
OP	76.20	93.04	0.01784	0.04811	0.000332	0.93979	0.31933	(1000, 50, 50, 1000)

Table 3. Calibration results for pretrained ResNet 152 on ImageNet.

Method	Top-1(%)	Top-5(%)	ECE	MCE	Brier	NLL	Classwise ECE	Architecture
Uncalibrated	77.05	93.46	0.05720	0.13071	0.000325	0.94395	0.31391	N/A
Temp. Scaling	77.05	93.46	0.01939	0.04937	0.000321	0.90930	0.30963	(1, 1)
Dir-ODIR	76.43	93.38	0.05146	0.11846	0.000333	0.95125	0.32609	(1000, 1000)
MS-ODIR	76.45	93.34	0.05026	0.10883	0.000332	0.94928	0.32502	(1000, 1000)
DIAGONAL	77.05	93.46	0.01365	0.05992	0.000319	0.89025	0.31578	(1, 10, 1)
OI	77.05	93.46	0.02075	0.06910	0.000322	0.91099	0.31402	(1000, 100, 100, 1000)
OP	77.05	93.46	0.01467	0.06734	0.000321	0.91050	0.30942	(1000, 50, 50, 1000)

Table 4. Calibration results for pretrained DenseNet 161 on ImageNet.

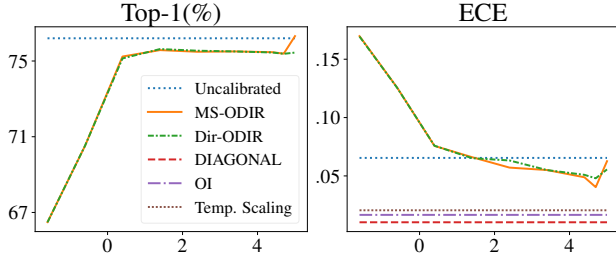


Figure 4. MS-ODIR and Dir-ODIR performance vs. regularization weight on ResNet 152, ImageNet. In the left (right) plot, x-axis shows the log scale regularization and y-axis shows the accuracy (ECE) of different methods. We keep the regularization weight of the bias parameter constant for this experiment. A high regularization value $\lambda > 10^4$ is required to achieve the best ECE while the transformation still loses about 1% accuracy compared to the original model.

1000 classes. We use the public pretrained models³ and split the validation dataset into calibration and test datasets for this experiment. As (Kull et al., 2019) have not provided results for the ImageNet dataset, we use the official code published by the author to report the results on this dataset. Note that the size of calibration dataset is relatively small with respect to the number of classes; thus we would expect that the choice of regularization is critical in this experiment.

Table 3 and Table 4 present the calibration performance as well as the top- k accuracy of different methods on ResNet 152 and DenseNet 161 models, respectively. The last column in both tables shows the selected architecture of each method. The number of units in each layer are

represented by a sequence of numbers, e.g. (10, 20, 30, 40) represents a network with 10 input units, 20 and 30 units in the first and second hidden layers, respectively, and 40 output units. In addition to the metrics we discussed in Section 2.1, we report calibration performance in classwise ECE (the multi-class extension of ECE) (Kull et al., 2019).

Overall, DIAGONAL again outperforms all the other baselines. As shown in Fig. 3, DIAGONAL learns an optimal transformation with few hundreds parameters. OI is the second best in ECE and Brier measures, the best MCE using ResNet 152, and slightly worse than temperature scaling and OP on the DenseNet model.

Lastly, MS-ODIR and Dir-ODIR performances are inferior to other methods in both accuracy and calibration. Because the number of parameters for MS-ODIR and Dir-ODIR methods grows quadratically with the number of classes, maintaining high accuracy as well as good calibration performance becomes harder. As shown in Fig. 4, we have to highly regularize the off diagonal weights to avoid losing much in accuracy in these methods. This high regularization limits the capability of the model to learn calibration maps.

7. Conclusion

In this work, we introduce the family of intra order-preserving functions which retain the top- k predictions of any deep network when used as the post-hoc calibration function. We propose a new neural network architecture to represent these functions, and new regularization techniques based on order-invariant and diagonal structures. In short, calibrating neural network with this new family of

³https://github.com/markus93/NN_calibration

functions generalizes many existing calibration techniques, with additional flexibility to express the post-hoc calibration function. The experimental results show the importance of learning within the intra order-preserving family as well as support the effectiveness of the proposed regularization in calibrating multiple classifiers on various datasets.

References

- Brier, G. W. Verification of forecasts expressed in terms of probability. *Monthly weather review*, 78(1):1–3, 1950.
- Cao, Z., Simon, T., Wei, S.-E., and Sheikh, Y. Realtime multi-person 2d pose estimation using part affinity fields. In *CVPR*, 2017.
- Caruana, R., Lou, Y., Gehrke, J., Koch, P., Sturm, M., and Elhadad, N. Intelligible models for healthcare: Predicting pneumonia risk and hospital 30-day readmission. In *Proceedings of the 21th ACM SIGKDD international conference on knowledge discovery and data mining*, pp. 1721–1730, 2015.
- Clenshaw, C. W. and Curtis, A. R. A method for numerical integration on an automatic computer. *Numerische Mathematik*, 2(1):197–205, 1960.
- Deng, J., Dong, W., Socher, R., Li, L.-J., Li, K., and Fei-Fei, L. Imagenet: A large-scale hierarchical image database. In *2009 IEEE conference on computer vision and pattern recognition*, pp. 248–255. Ieee, 2009.
- Facchinei, F. and Pang, J.-S. *Finite-dimensional variational inequalities and complementarity problems*. Springer Science & Business Media, 2007.
- Gal, Y. and Ghahramani, Z. Dropout as a bayesian approximation: Representing model uncertainty in deep learning. In *international conference on machine learning*, pp. 1050–1059, 2016.
- Girshick, R. Fast r-cnn. In *Proceedings of the IEEE international conference on computer vision*, pp. 1440–1448, 2015.
- Guo, C., Pleiss, G., Sun, Y., and Weinberger, K. Q. On calibration of modern neural networks. In *Proceedings of the 34th International Conference on Machine Learning-Volume 70*, pp. 1321–1330. JMLR. org, 2017.
- He, K., Zhang, X., Ren, S., and Sun, J. Deep residual learning for image recognition. In *Proceedings of the IEEE conference on computer vision and pattern recognition*, pp. 770–778, 2016.
- Huang, G., Liu, Z., Van Der Maaten, L., and Weinberger, K. Q. Densely connected convolutional networks. In *Proceedings of the IEEE conference on computer vision and pattern recognition*, pp. 4700–4708, 2017.
- Huber, P. J. Robust estimation of a location parameter. In *Breakthroughs in statistics*, pp. 492–518. Springer, 1992.
- Jiang, X., Osl, M., Kim, J., and Ohno-Machado, L. Calibrating predictive model estimates to support personalized medicine. *Journal of the American Medical Informatics Association*, 19(2):263–274, 2012.
- Kendall, A. and Gal, Y. What uncertainties do we need in bayesian deep learning for computer vision? In *Advances in neural information processing systems*, pp. 5574–5584, 2017.
- Kingma, D. P. and Ba, J. Adam: A method for stochastic optimization. In *ICLR*, 2014.
- Krizhevsky, A., Hinton, G., et al. Learning multiple layers of features from tiny images. 2009.
- Kull, M., Silva Filho, T., and Flach, P. Beta calibration: a well-founded and easily implemented improvement on logistic calibration for binary classifiers. In *Artificial Intelligence and Statistics*, pp. 623–631, 2017a.
- Kull, M., Silva Filho, T. M., Flach, P., et al. Beyond sigmoids: How to obtain well-calibrated probabilities from binary classifiers with beta calibration. *Electronic Journal of Statistics*, 11(2):5052–5080, 2017b.
- Kull, M., Nieto, M. P., Kängsepp, M., Silva Filho, T., Song, H., and Flach, P. Beyond temperature scaling: Obtaining well-calibrated multi-class probabilities with dirichlet calibration. In *Advances in Neural Information Processing Systems*, pp. 12295–12305, 2019.
- Kumar, A., Sarawagi, S., and Jain, U. Trainable calibration measures for neural networks from kernel mean embeddings. In *International Conference on Machine Learning*, pp. 2805–2814, 2018.
- Liu, D. C. and Nocedal, J. On the limited memory bfgs method for large scale optimization. *Mathematical programming*, 45(1-3):503–528, 1989.
- Maddox, W. J., Izmailov, P., Garipov, T., Vetrov, D. P., and Wilson, A. G. A simple baseline for bayesian uncertainty in deep learning. In *Advances in Neural Information Processing Systems*, pp. 13132–13143, 2019.
- Mozafari, A. S., Gomes, H. S., Leão, W., and Gagné, C. Unsupervised temperature scaling: Post-processing unsupervised calibration of deep models decisions. 2019.
- Müller, R., Kornblith, S., and Hinton, G. E. When does label smoothing help? In *Advances in Neural Information Processing Systems*, pp. 4696–4705, 2019.

- Naeini, M. P., Cooper, G., and Hauskrecht, M. Obtaining well calibrated probabilities using bayesian binning. In *Twenty-Ninth AAAI Conference on Artificial Intelligence*, 2015.
- Netzer, Y., Wang, T., Coates, A., Bissacco, A., Wu, B., and Ng, A. Y. Reading digits in natural images with unsupervised feature learning. 2011.
- Nixon, J., Dusenberry, M., Zhang, L., Jerfel, G., and Tran, D. Measuring calibration in deep learning. *arXiv preprint arXiv:1904.01685*, 2019.
- Pereyra, G., Tucker, G., Chorowski, J., Kaiser, Ł., and Hinton, G. Regularizing neural networks by penalizing confident output distributions. *arXiv preprint arXiv:1701.06548*, 2017.
- Platt, J. et al. Probabilistic outputs for support vector machines and comparisons to regularized likelihood methods. *Advances in large margin classifiers*, 10(3):61–74, 1999.
- Ren, S., He, K., Girshick, R., and Sun, J. Faster r-cnn: Towards real-time object detection with region proposal networks. In *Advances in neural information processing systems*, pp. 91–99, 2015.
- Seo, S., Seo, P. H., and Han, B. Learning for single-shot confidence calibration in deep neural networks through stochastic inferences. In *Proceedings of the IEEE Conference on Computer Vision and Pattern Recognition*, pp. 9030–9038, 2019.
- Thulasidasan, S., Chennupati, G., Bilmes, J. A., Bhattacharya, T., and Michalak, S. On mixup training: Improved calibration and predictive uncertainty for deep neural networks. In *Advances in Neural Information Processing Systems*, pp. 13888–13899, 2019.
- Wehenkel, A. and Louppe, G. Unconstrained monotonic neural networks. In *Advances in Neural Information Processing Systems*, pp. 1543–1553, 2019.
- Xing, C., Arik, S., Zhang, Z., and Pfister, T. Distance-based learning from errors for confidence calibration. In *International Conference on Learning Representations*, 2020.
- Yun, S., Han, D., Oh, S. J., Chun, S., Choe, J., and Yoo, Y. Cutmix: Regularization strategy to train strong classifiers with localizable features. In *Proceedings of the IEEE International Conference on Computer Vision*, pp. 6023–6032, 2019.
- Zadrozny, B. and Elkan, C. Obtaining calibrated probability estimates from decision trees and naive bayesian classifiers. In *Icml*, volume 1, pp. 609–616. Citeseer, 2001.
- Zadrozny, B. and Elkan, C. Transforming classifier scores into accurate multiclass probability estimates. In *Proceedings of the eighth ACM SIGKDD international conference on Knowledge discovery and data mining*, pp. 694–699, 2002.
- Zagoruyko, S. and Komodakis, N. Wide residual networks. In *BMVC*, 2016.
- Zhang, H., Cissé, M., Dauphin, Y. N., and Lopez-Paz, D. mixup: Beyond empirical risk minimization. In *6th International Conference on Learning Representations, ICLR 2018*, 2018.

A. Missing Proofs

A.1. Proof of Theorem 1, Intra Order-preserving Functions

Theorem 1. A continuous function $\mathbf{f} : \mathbb{R}^n \rightarrow \mathbb{R}^n$ is intra order-preserving, if and only if $\mathbf{f}(\mathbf{x}) = S(\mathbf{x})^{-1}U\mathbf{w}(\mathbf{x})$ with U being an upper-triangular matrix of ones and $\mathbf{w} : \mathbb{R}^n \rightarrow \mathbb{R}^n$ being a continuous function such that

- $\mathbf{w}_i(\mathbf{x}) = 0$, if $\mathbf{y}_i = \mathbf{y}_{i+1}$ and $i < n$,
- $\mathbf{w}_i(\mathbf{x}) > 0$, if $\mathbf{y}_i > \mathbf{y}_{i+1}$ and $i < n$,
- $\mathbf{w}_n(\mathbf{x})$ is arbitrary,

where $\mathbf{y} = S(\mathbf{x})\mathbf{x}$ is the sorted version of \mathbf{x} .

Proof of Theorem 1. (\rightarrow) For a continuous intra order-preserving function $\mathbf{f}(\mathbf{x})$, let $\mathbf{w}(\mathbf{x}) = U^{-1}S(\mathbf{x})\mathbf{f}(\mathbf{x})$. First we show \mathbf{w} is continuous. Because \mathbf{f} is intra order-preserving, it holds that $S(\mathbf{x}) = S(\mathbf{f}(\mathbf{x}))$. Let $\hat{\mathbf{f}}(\mathbf{x}) := S(\mathbf{f}(\mathbf{x}))\mathbf{f}(\mathbf{x})$ be the sorted version of $\mathbf{f}(\mathbf{x})$. The above implies $\mathbf{w}(\mathbf{x}) = U^{-1}\hat{\mathbf{f}}(\mathbf{x})$. By Lemma 1, we know $\hat{\mathbf{f}}$ is continuous and therefore \mathbf{w} is also continuous.

Lemma 1. Let $\mathbf{f} : \mathbb{R}^n \rightarrow \mathbb{R}^n$ be a continuous intra order-preserving function. $S(\mathbf{f}(\mathbf{x}))\mathbf{f}(\mathbf{x})$ is a continuous function.

Next, we show that \mathbf{w} satisfies the properties listed in Theorem 1. As $\mathbf{w}(\mathbf{x}) = U^{-1}\hat{\mathbf{f}}(\mathbf{x})$, we can equivalently write \mathbf{w} as

$$\mathbf{w}_i(\mathbf{x}) = \begin{cases} \hat{\mathbf{f}}_i(\mathbf{x}) - \hat{\mathbf{f}}_{i+1}(\mathbf{x}) & 1 \leq i < n \\ \hat{\mathbf{f}}_n(\mathbf{x}) & i = n. \end{cases}$$

Since $\hat{\mathbf{f}}$ is the sorted version of \mathbf{f} , it holds that $\mathbf{w}_i(\mathbf{x}) \geq 0$ for $1 \leq i < n$. Also, by the definition of the order-preserving function, $\mathbf{w}_i(\mathbf{x})$ can be zero if and only if $\mathbf{y}_i = \mathbf{y}_{i+1}$, where $\mathbf{y} = S(\mathbf{x})\mathbf{x}$. These two arguments prove the necessary condition.

(\leftarrow) For a given $\mathbf{w}(\mathbf{x})$ satisfying the condition in the theorem statement, let $\mathbf{v}(\mathbf{x}) = U\mathbf{w}(\mathbf{x})$. Equivalently, we can write $\mathbf{v}_i(\mathbf{x}) = \sum_{j=0}^{n-i} \mathbf{w}_{n-j}(\mathbf{x})$ and $\mathbf{v}_i(\mathbf{x}) - \mathbf{v}_{i+1}(\mathbf{x}) = \mathbf{w}_i(\mathbf{x})$, $\forall i \in [n]$. By construction of \mathbf{w} , one can conclude that $\mathbf{v}(\mathbf{x})$ is a sorted vector where two consecutive elements $\mathbf{v}_i(\mathbf{x})$ and $\mathbf{v}_{i+1}(\mathbf{x})$ are equal if and only if $\mathbf{y}_i = \mathbf{y}_{i+1}$. Therefore, $\mathbf{f}(\mathbf{x}) = S(\mathbf{x})^{-1}\mathbf{v}(\mathbf{x})$ has the same ranking as \mathbf{x} . In other words, \mathbf{f} is an intra order-preserving function. The continuity of \mathbf{f} follows from the lemma below and the fact that \mathbf{v} is continuous when \mathbf{w} is continuous. Lemma 2.

Lemma 2. Let $\mathbf{v} : \mathbb{R}^n \rightarrow \mathbb{R}^n$ be a continuous function in which $\mathbf{v}_i(\mathbf{x})$ and $\mathbf{v}_{i+1}(\mathbf{x})$ are equal if and only if $\mathbf{y}_i = \mathbf{y}_{i+1}$, where $\mathbf{y} = S(\mathbf{x})\mathbf{x}$. Then $\mathbf{f}(\mathbf{x}) = S(\mathbf{x})^{-1}\mathbf{v}(\mathbf{x})$ is a continuous function. ■

A.1.1. DEFERRED PROOFS OF LEMMAS

Proof of Lemma 1. Let $\mathbb{P}^n = \{P_1, \dots, P_K\}$ be the finite set of all possible $n \times n$ dimensional permutation matrices. For each $k \in [K]$, define the closed set $\mathbb{N}_k = \{\mathbf{x} : S(\mathbf{x})\mathbf{x} = P_k\mathbf{x}\}$. These sets are convex polyhedrons since each can be defined by a finite set of linear inequalities; in addition, they together form a covering set of \mathbb{R}^n . Note that $S(\mathbf{x}) = P_k$ is constant in the interior $\text{int}(\mathbb{N}_k)$, but $S(\mathbf{x})$ may change on the boundary $\partial(\mathbb{N}_k)$ which corresponds to points where a tie exists in elements of \mathbf{x} (for such a point $S(\mathbf{x}) \neq P_k$). Nonetheless, by definition of the set \mathbb{N}_k , we have $S(\mathbf{x})\mathbf{x} = P_k\mathbf{x}$ for all $\mathbf{x} \in \mathbb{N}_k$, which implies that $S(\mathbf{x})$ and P_k can only have different elements for indices where elements of \mathbf{x} are equal.

To prove that $\hat{\mathbf{f}}(\mathbf{x}) := S(\mathbf{f}(\mathbf{x}))\mathbf{f}(\mathbf{x})$ is continuous, we leverage the fact that $\hat{\mathbf{f}}(\mathbf{x}) = S(\mathbf{x})\mathbf{f}(\mathbf{x})$ for intra order-preserving \mathbf{f} . We will first show that $\hat{\mathbf{f}}(\mathbf{x}) = P_k\mathbf{f}(\mathbf{x})$ for $\mathbf{x} \in \mathbb{N}_k$ and any $k \in [K]$, which implies $\hat{\mathbf{f}}$ is continuous on \mathbb{N}_k when \mathbf{f} is continuous. To see this, consider an arbitrary $k \in [K]$. For $\mathbf{x} \in \text{int}(\mathbb{N}_k)$ in the interior, we have $S(\mathbf{x}) = P_k$ and therefore $\hat{\mathbf{f}}(\mathbf{x}) = P_k\mathbf{f}(\mathbf{x})$. For $\mathbf{x} \in \partial\mathbb{N}_k$ on the boundary, we have

$$\hat{\mathbf{f}}(\mathbf{x}) = S(\mathbf{x})\mathbf{f}(\mathbf{x}) = P_k\mathbf{f}(\mathbf{x}).$$

The last equality holds because the difference between $S(\mathbf{x})$ and P_k are only in the indices for which elements of \mathbf{x} are equal, and the order-preserving \mathbf{f} preserves exactly the same equalities. Thus, the differences between permutations $S(\mathbf{x})$ and P_k do not reflect in the products $S(\mathbf{x})\mathbf{f}(\mathbf{x})$ and $P_k\mathbf{f}(\mathbf{x})$.

Next, we show that $\hat{\mathbf{f}}(\mathbf{x}) = P_k\mathbf{f}(\mathbf{x}) = P_{k'}\mathbf{f}(\mathbf{x})$ for $\mathbf{x} \in \partial\mathbb{N}_k \cap \partial\mathbb{N}_{k'}$. While $P_k \neq P_{k'}$, the intersection $\partial\mathbb{N}_k \cap \partial\mathbb{N}_{k'}$ contains exactly points \mathbf{x} such that the index differences in P_k and $P_{k'}$ correspond to same value in \mathbf{x} . Because \mathbf{f} is order-preserving, by an argument similar to the previous step, we have $P_k\mathbf{f}(\mathbf{x}) = P_{k'}\mathbf{f}(\mathbf{x})$ for $\mathbf{x} \in \partial\mathbb{N}_k \cap \partial\mathbb{N}_{k'}$.

Together these two steps and the fact that $\{\mathbb{N}_k\}$ is covering set on \mathbb{R}^n show that $\hat{\mathbf{f}}$ is a piece-wise continuous function on \mathbb{R}^n when \mathbf{f} is continuous on \mathbb{R}^n . ■

Proof of Lemma 2. In order to show the continuity of $\mathbf{f}(\mathbf{x})$, we use a similar argument as in Lemma 1 (see therein for notation definitions). For any $k \in [K]$, it is also trivial to show that \mathbf{f} is continuous over the open set $\text{int}(\mathbb{N}_k)$ since $\mathbf{f}(\mathbf{x}) = P_k^{-1}\mathbf{v}(\mathbf{x})$. We use the same argument as Lemma 1 to show it is also a continuous for any point $\mathbf{x} \in \partial(\mathbb{N}_k)$

$$\mathbf{f}(\mathbf{x}) = S(\mathbf{x})^{-1}\mathbf{v}(\mathbf{x}) = P_k^{-1}\mathbf{v}(\mathbf{x}).$$

The last equality holds because P_k^{-1} and $S(\mathbf{x})^{-1}$ can only have different elements among elements of $\mathbf{y} = S(\mathbf{x})\mathbf{x}$ with equal values, and \mathbf{v} preserves exactly these equalities in \mathbf{y} . Finally, the proof can be completed by piecing the results of different \mathbb{N}_k together. ■

A.2. Proof of Theorem 2, Order-invariant Functions

Theorem 2. A continuous, intra order-preserving function $\mathbf{f} : \mathbb{R}^n \rightarrow \mathbb{R}^n$ is order invariant, if and only if $\mathbf{f}(\mathbf{x}) = S(\mathbf{x})^{-1}U\mathbf{w}(\mathbf{y})$, where U , \mathbf{w} , and \mathbf{y} are in Theorem 1.

To prove Theorem 2, we first study the properties of order invariant functions in Appendix A.2.1. We will provide necessary and sufficient conditions to describe order invariant functions, like what we did in Theorem 1 for intra order-preserving functions. Finally, we combine these insights and Theorem 1 to prove Theorem 2 in Appendix A.2.2.

A.2.1. PROPERTIES OF ORDER INVARIANT FUNCTIONS

The goal of this section is to prove the below theorem, which characterizes the representation of order invariant functions using the concept of equality-preserving.

Definition 6. We say a function $\mathbf{f} : \mathbb{R}^n \rightarrow \mathbb{R}^n$ is *equality-preserving*, if $\mathbf{f}_i(\mathbf{x}) = \mathbf{f}_j(\mathbf{x})$ for all $\mathbf{x} \in \mathbb{R}^n$ such that $\mathbf{x}_i = \mathbf{x}_j$ for some $i, j \in [n]$

Theorem 4. A function $\mathbf{f} : \mathbb{R}^n \rightarrow \mathbb{R}^n$ is order-invariant, if and only if $\mathbf{f}(\mathbf{x}) = S(\mathbf{x})^{-1}\bar{\mathbf{f}}(S(\mathbf{x})\mathbf{x})$ for some function $\bar{\mathbf{f}} : \mathbb{R}^n \rightarrow \mathbb{R}^n$ that is equality-preserving on the domain $\{\mathbf{y} : \mathbf{y} = S(\mathbf{x})\mathbf{x}, \text{ for } \mathbf{x} \in \mathbb{R}^n\}$.

Theorem 4 shows an order invariant function can be expressed in terms of some equality-preserving function. In fact, every order invariant function is equality-preserving.

Proposition 1. Any order-invariant function $\mathbf{f} : \mathbb{R}^n \rightarrow \mathbb{R}^n$ is equality-preserving.

Proof. Let $P_{ij} \in \mathbb{P}^n$ denote the permutation matrix that only swaps i^{th} and j^{th} elements of the input vector; i.e. $\mathbf{y} = P_{ij}\mathbf{x} \Rightarrow \mathbf{y}_i = \mathbf{x}_j, \mathbf{y}_j = \mathbf{x}_i, \mathbf{y}_k = \mathbf{x}_k, \forall \mathbf{x} \in \mathbb{R}^n, i, j, k \in [n]$, and $k \neq i, j$. Thus, for an order-invariant function $\mathbf{f} : \mathbb{R}^n \rightarrow \mathbb{R}^n$ and any $\mathbf{x} \in \mathbb{R}^n$ such that $\mathbf{x}_i = \mathbf{x}_j$, we have

$$\mathbf{f}(P_{ij}\mathbf{x}) = P_{ij}\mathbf{f}(\mathbf{x}) \Rightarrow \mathbf{f}_i(P_{ij}\mathbf{x}) = \mathbf{f}_j(\mathbf{x}) \Rightarrow \mathbf{f}_i(\mathbf{x}) = \mathbf{f}_j(\mathbf{x}) \quad (\because P_{ij}\mathbf{x} = \mathbf{x} \text{ for } \mathbf{x} \text{ such that } \mathbf{x}_i = \mathbf{x}_j).$$

We are almost ready to prove Theorem 4. We just need one more technical lemma, whose proof is deferred to the end of this section.

Lemma 3. For any $P \in \mathbb{P}^n$ and an equality-preserving $\mathbf{f} : \mathbb{R}^n \rightarrow \mathbb{R}^n$, $S(\mathbf{x})\mathbf{f}(\mathbf{x}) = S(P\mathbf{x})P\mathbf{f}(\mathbf{x})$.

Proof of Theorem 4. (\rightarrow) For an order-invariant function $\mathbf{f} : \mathbb{R}^n \rightarrow \mathbb{R}^n$, we have $\mathbf{f}(P\mathbf{x}) = P\mathbf{f}(\mathbf{x})$ by Definition 3 for any $P \in \mathbb{P}^n$. Take $P = S(\mathbf{x})$. We then have the equality $\mathbf{f}(\mathbf{x}) = S(\mathbf{x})^{-1}\mathbf{f}(S(\mathbf{x})\mathbf{x})$. This is an admissible representation because, by Proposition 1, \mathbf{f} is equality-preserving.

(\leftarrow) Let $\mathbf{f}(\mathbf{x}) = S(\mathbf{x})^{-1}\bar{\mathbf{f}}(S(\mathbf{x})\mathbf{x})$ for some equality-preserving function $\bar{\mathbf{f}}$. First, because $\bar{\mathbf{f}}$ is equality preserving and \mathbf{f} is constructed through the sorting function S , we notice that $\mathbf{f}(\mathbf{x})$ is equality-preserving. Next, we show \mathbf{f} is also order invariant:

$$\begin{aligned} \mathbf{f}(P\mathbf{x}) &= S(P\mathbf{x})^{-1}\bar{\mathbf{f}}(S(P\mathbf{x})P\mathbf{x}) \\ &= S(P\mathbf{x})^{-1}\bar{\mathbf{f}}(S(\mathbf{x})\mathbf{x}) && (\because S(P\mathbf{x})P\mathbf{x} = S(\mathbf{x})\mathbf{x} \text{ by choosing } \mathbf{f}(\mathbf{x}) = \mathbf{x} \text{ in Lemma 3}) \\ &= S(P\mathbf{x})^{-1}S(\mathbf{x})\mathbf{f}(\mathbf{x}) && (\because \text{definition of } \mathbf{f}(\mathbf{x})) \\ &= S(P\mathbf{x})^{-1}S(P\mathbf{x})P\mathbf{f}(\mathbf{x}) && (\because \text{Lemma 3}) \\ &= P\mathbf{f}(\mathbf{x}). \end{aligned}$$

A.2.2. MAIN PROOF

Proof of Theorem 2. (\rightarrow) From Theorem 1 we can write $\mathbf{f}(\mathbf{x}) = S(\mathbf{x})^{-1}U\mathbf{w}(\mathbf{x})$. On the other hand, from Theorem 4 we can write $\mathbf{f}(\mathbf{x}) = S(\mathbf{x})^{-1}\bar{\mathbf{f}}(\mathbf{y})$ for some equality-preserving function $\bar{\mathbf{f}}$. Using both we can identify $\mathbf{w}(\mathbf{x}) = U^{-1}\bar{\mathbf{f}}(\mathbf{y})$ which implies that \mathbf{w} is only a function of the sorted input \mathbf{y} and can be equivalently written as $\mathbf{w}(\mathbf{y})$.

(\leftarrow) For \mathbf{w} with the properties in the theorem statement, the function $\mathbf{f}(\mathbf{x}) = S(\mathbf{x})^{-1}U\mathbf{w}(\mathbf{y})$ satisfies the conditions of Theorem 1; therefore \mathbf{f} is intra order-preserving. To show \mathbf{f} is also order-invariant, we write $\mathbf{f}(\mathbf{x}) = S(\mathbf{x})^{-1}\bar{\mathbf{f}}(\mathbf{y})$ where $\bar{\mathbf{f}}(\mathbf{y}) = U\mathbf{w}(\mathbf{y})$. Because $\bar{\mathbf{f}}_i(\mathbf{y}) = \sum_{j=0}^{n-i} \mathbf{w}_{n-j}(\mathbf{x})$, we can derive with the definition of \mathbf{w} that

$$\mathbf{y}_i = \mathbf{y}_{i+1} \Rightarrow \mathbf{w}_i(\mathbf{y}) = 0 \Rightarrow \bar{\mathbf{f}}_i(\mathbf{x}) = \bar{\mathbf{f}}_{i+1}(\mathbf{x}).$$

That is, $\bar{\mathbf{f}}(\mathbf{y})$ is equality-preserving on the domain of sorted inputs. Thus, \mathbf{f} is also order-invariant. \blacksquare

A.2.3. DEFERRED PROOF OF LEMMAS

Proof of Lemma 3. To prove the statement, we first notice a fact that $S(\mathbf{x}) = S(P\mathbf{x})P$, for any $P \in \mathbb{P}^n$ and $\mathbf{x} \in \mathbb{X} := \{\mathbf{x} \in \mathbb{R}^n : \mathbf{x}_i \neq \mathbf{x}_j, \forall i, j \in [n], i \neq j\}$. Therefore, for $\mathbf{x} \in \mathbb{X}$, we have $S(\mathbf{x})\mathbf{f}(\mathbf{x}) = S(P\mathbf{x})P\mathbf{f}(\mathbf{x})$.

Otherwise, consider some $\mathbf{x} \in \mathbb{R}^n \setminus \mathbb{X}$. Without loss of generality⁴, we may consider $n > 2$ and \mathbf{x} such that $\mathbf{x}_1 = \mathbf{x}_2 > \mathbf{x}_k$ for all $k > 2$; because \mathbf{f} is equality-preserving, we have $\mathbf{f}_1(\mathbf{x}) = \mathbf{f}_2(\mathbf{x})$.

To prove the desired equality, we will introduce some extra notations. We use subscript $i:j$ to extract contiguous parts of a vector, e.g. $\mathbf{x}_{2:n} = [\mathbf{x}_2, \dots, \mathbf{x}_n]$ and $\mathbf{f}_{2:n}(\mathbf{x}) = [\mathbf{f}_2(\mathbf{x}), \dots, \mathbf{f}_n(\mathbf{x})]$ (by our construction of \mathbf{x} , $\mathbf{x}_{2:n}$ is a vector where each element is unique.) In addition, without loss of generality, suppose $P \in \mathbb{P}^n$ shifts index 1 to some index $i \in [n]$; we define $\bar{P} \in \{0, 1\}^{n-1 \times n-1}$ by removing the 1st column and the i th row of P (which is also a permutation matrix). Using this notion, we can partition $S(\bar{P}\mathbf{x}_{2:n}) \in \{0, 1\}^{n-1 \times n-1}$ as

$$S(\bar{P}\mathbf{x}_{2:n}) = \begin{bmatrix} B_1 & B_2 \\ B_3 & B_4 \end{bmatrix}$$

where $B_1 \in \mathbb{R}^{1 \times i-1}$, $B_2 \in \mathbb{R}^{1 \times n-i}$, $B_3 \in \mathbb{R}^{n-2 \times i-1}$, and $B_4 \in \mathbb{R}^{n-2 \times n-i}$. This would imply that $S(P\mathbf{x}) \in \{0, 1\}^{n \times n}$ can be written as one of followings

$$\begin{bmatrix} e_i^\top & & \\ B_1 & 0 & B_2 \\ B_3 & 0 & B_4 \end{bmatrix} \quad \text{or} \quad \begin{bmatrix} B_1 & 0 & B_2 \\ & e_i^\top & \\ B_3 & 0 & B_4 \end{bmatrix} \quad (4)$$

where e_i is the i th canonical basis.

⁴This choice is only for convenience of writing the indices.

To prove the statement, let $\mathbf{y} = P\mathbf{f}(\mathbf{x})$. By the definition of \bar{P} , we can also write \mathbf{y} as

$$\mathbf{y} = \begin{bmatrix} \mathbf{y}_{1:i-1} \\ \mathbf{y}_i \\ \mathbf{y}_{i+1:n} \end{bmatrix} = \begin{bmatrix} (\bar{P}\mathbf{f}_{2:n}(\mathbf{x}))_{1:i-1} \\ \mathbf{f}_1(\mathbf{x}) \\ (\bar{P}\mathbf{f}_{2:n}(\mathbf{x}))_{i:n-1} \end{bmatrix} \quad (5)$$

Let us consider the first case in (4). We have

$$S(P\mathbf{x})P\mathbf{f}(\mathbf{x}) = \begin{bmatrix} \mathbf{y}_i \\ B_1\mathbf{y}_{1:i-1} + B_2\mathbf{y}_{i+1:n} \\ B_3\mathbf{y}_{1:i-1} + B_4\mathbf{y}_{i+1:n} \end{bmatrix} = \begin{bmatrix} \mathbf{y}_i \\ S(\bar{P}\mathbf{x}_{2:n})\bar{P}\mathbf{f}_{2:n}(\mathbf{x}) \end{bmatrix} = \begin{bmatrix} \mathbf{f}_1(\mathbf{x}) \\ S(\mathbf{x}_{2:n})\mathbf{f}_{2:n}(\mathbf{x}) \end{bmatrix} = S(\mathbf{x})\mathbf{f}(\mathbf{x})$$

where the second equality follows from (5), the third from the fact we proved at the beginning for the set \mathbb{X} , and the last equality is due to the assumption $\mathbf{x}_1 = \mathbf{x}_2 > \mathbf{x}_k$ and the equality-preserving property that $\mathbf{f}_1(\mathbf{x}) = \mathbf{f}_2(\mathbf{x})$. For the second case in (4), based on the same reasoning above, we can show

$$S(P\mathbf{x})P\mathbf{f}(\mathbf{x}) = \begin{bmatrix} (S(\mathbf{x}_{2:n})\mathbf{f}_{2:n}(\mathbf{x}))_1 \\ \mathbf{f}_1(\mathbf{x}) \\ (S(\mathbf{x}_{2:n})\mathbf{f}_{2:n}(\mathbf{x}))_{2:n-1} \end{bmatrix},$$

Because $\mathbf{x}_1 = \mathbf{x}_2$, we have $(S(\mathbf{x}_{2:n})\mathbf{f}_{2:n}(\mathbf{x}))_1 = \mathbf{f}_1(\mathbf{x}) = \mathbf{f}_2(\mathbf{x})$. Thus, $S(P\mathbf{x})P\mathbf{f}(\mathbf{x}) = S(\mathbf{x})\mathbf{x}$. ■

A.3. Proof of Theorem 3, Diagonal Functions

Theorem 3. A continuous, intra order-preserving function $\mathbf{f} : \mathbb{R}^n \rightarrow \mathbb{R}^n$ is diagonal, if and only if $\mathbf{f}(\mathbf{x}) = [\bar{f}(\mathbf{x}_1), \dots, \bar{f}(\mathbf{x}_n)]$ for some continuous and increasing function $\bar{f} : \mathbb{R} \rightarrow \mathbb{R}$.

We first prove some properties of *diagonal* intra order-preserving functions, which will be used to prove Theorem 3.

Proposition 2. Any intra order-preserving function $\mathbf{f} : \mathbb{R}^n \rightarrow \mathbb{R}^n$ is equality-preserving.

Proof. This can be seen directly from the definition of intra order-preserving functions. ■

Corollary 2. The following statements are equivalent

1. A function $\mathbf{f} : \mathbb{R}^n \rightarrow \mathbb{R}^n$ is diagonal and equality-preserving.
2. $\mathbf{f}(\mathbf{x}) = [\bar{f}(\mathbf{x}_1), \dots, \bar{f}(\mathbf{x}_n)]$ for some $\bar{f} : \mathbb{R} \rightarrow \mathbb{R}$.
3. A function $\mathbf{f} : \mathbb{R}^n \rightarrow \mathbb{R}^n$ is diagonal and order-invariant.

Proof. (1 \rightarrow 2) Let $\mathbf{f}(\mathbf{x}) = [f_1(\mathbf{x}_1), \dots, f_n(\mathbf{x}_n)]$ be a diagonal and equality-preserving function. One can conclude that $\mathbf{f}_1(x) = \dots = \mathbf{f}_n(x)$ for all $x \in \mathbb{R}$.

(2 \rightarrow 3) Let $\mathbf{u} = P\mathbf{x}$ for some permutation matrix $P \in \mathbb{P}^n$. Then $\mathbf{f}(P\mathbf{x}) = [\bar{f}(\mathbf{u}_1), \dots, \bar{f}(\mathbf{u}_n)] = P[\bar{f}(\mathbf{x}_1), \dots, \bar{f}(\mathbf{x}_n)] = P\mathbf{f}(\mathbf{x})$.

(3 \rightarrow 1) True by Proposition 1. ■

Proof of Theorem 3. (\rightarrow) By Proposition 2, an intra order-preserving function \mathbf{f} is also equality-preserving. Therefore, by Corollary 2 it can be represented in the form $\mathbf{f}(\mathbf{x}) = [\bar{f}(\mathbf{x}_1), \dots, \bar{f}(\mathbf{x}_n)]$ for some $\bar{f} : \mathbb{R} \rightarrow \mathbb{R}$. Furthermore, because $\mathbf{f}(\mathbf{x})$ is intra order-preserving, for any $\mathbf{x} \in \mathbb{R}^n$ with $\mathbf{x}_1 > \mathbf{x}_2$, it satisfies $\mathbf{f}_1(\mathbf{x}_1) > \mathbf{f}_2(\mathbf{x}_2)$; that is, $\bar{f}(\mathbf{x}_1) > \bar{f}(\mathbf{x}_2)$. Therefore, \bar{f} is an increasing function. Continuity is inherited naturally.

(\leftarrow) Because $\mathbf{f}_i(\mathbf{x}) = \bar{f}(\mathbf{x}_i)$ and \bar{f} is an increasing function, it follows that \mathbf{f} is intra order-preserving

$$\mathbf{x}_i = \mathbf{x}_j \Rightarrow \mathbf{f}_i(\mathbf{x}) = \mathbf{f}_j(\mathbf{x}) \quad \text{and} \quad \mathbf{x}_i > \mathbf{x}_j \Rightarrow \mathbf{f}_i(\mathbf{x}) > \mathbf{f}_j(\mathbf{x}).$$
■

Finally, we prove that diagonal intra order-preserving functions are also order-invariant. This fact was mentioned in the paper without a proof.

Corollary 3. *A diagonal intra order-preserving function is also order-invariant.*

Proof. Intra order-preserving functions are equality-preserving by Proposition 2. By Corollary 2 an diagonal equality-preserving function is order-invariant. ■

B. Continuity and Differentiability of the Proposed Architecture

In this section, we discuss properties of the function $\mathbf{f}(\mathbf{x}) = S(\mathbf{x})^{-1}UD(\mathbf{y})\mathbf{m}(\mathbf{x})$. In order to learn the parameters of \mathbf{m} with a first order optimization algorithm, it is important for \mathbf{f} to be differentiable with respect to the parameters of \mathbf{m} . This condition holds in general, since the only potential sources of non-differentiable \mathbf{f} , $S(\mathbf{x})^{-1}$ and \mathbf{y} are constant with respect to the parameters of \mathbf{m} . Thus, if \mathbf{m} is differentiable with respect to its parameters, \mathbf{f} is also differentiable with respect to the parameters of \mathbf{m} .

Next, we discuss continuity and differentiability of $\mathbf{f}(\mathbf{x})$ with respect the *input* \mathbf{x} . These properties are important when the input to function f is first processed by a trainable function \mathbf{g} (i.e. the final output is computed as $\mathbf{f} \circ \mathbf{g}(\mathbf{x})$). This is not the case in post-hoc calibration considered in the paper, since the classifier \mathbf{g} here is not being trained in the calibration phase.

We show below that when $\mathbf{w}(\mathbf{x}) = D(\mathbf{y})\mathbf{m}(\mathbf{x})$ satisfies the requirements in Theorem 1, the function $\mathbf{f}(\mathbf{x}) = S(\mathbf{x})^{-1}UD(\mathbf{y})\mathbf{m}(\mathbf{x})$ is a continuous intra order-preserving function.

Corollary 4. *Let $\sigma : \mathbb{R} \rightarrow \mathbb{R}$ be a continuous function where $\sigma(0) = 0$ and strictly positive on $\mathbb{R} \setminus \{0\}$, and let \mathbf{m} be a continuous function where $\mathbf{m}_i(\mathbf{x}) > 0$ for $i < n$, and arbitrary for $\mathbf{m}_d(\mathbf{y})$. Let $D(\mathbf{y})$ denote a diagonal matrix with entries $D_{ii} = \sigma(\mathbf{y}_i - \mathbf{y}_{i+1})$ for $i < n$ and $D_{nn} = 1$. Then $\mathbf{w}(\mathbf{x}) = D(\mathbf{y})\mathbf{m}(\mathbf{x})$ is a continuous function and satisfies the following conditions*

- $\mathbf{w}_i(\mathbf{x}) = 0$, for $i < n$ and $\mathbf{y}_i = \mathbf{y}_{i+1}$
- $\mathbf{w}_i(\mathbf{x}) > 0$, for $i < n$ and $\mathbf{y}_i > \mathbf{y}_{i+1}$
- $\mathbf{w}_n(\mathbf{x})$ is arbitrary,

where $\mathbf{y} = S(\mathbf{x})\mathbf{x}$ is the sorted version of \mathbf{x} .

Proof. First, because $\mathbf{y} = S(\mathbf{x})\mathbf{x}$ is a continuous function (by Lemma 1 with $\mathbf{f}(\mathbf{x}) = \mathbf{x}$), $\mathbf{w}(\mathbf{x}) = D(\mathbf{y})\mathbf{m}(\mathbf{x})$ is also a continuous function. Second, because $\|\mathbf{x}\| < \infty$, we have $\mathbf{m}(\mathbf{x}) < \infty$ due to continuity. Therefore, it follows that $\mathbf{w}_i(\mathbf{x}) = \sigma(\mathbf{y}_i - \mathbf{y}_{i+1})\mathbf{m}_i(\mathbf{x})$ satisfies all the listed conditions. ■

To understand the differentiability of \mathbf{f} , we first see that \mathbf{f} may not be differentiable at a point where there is a tie among some elements of the input vector.

Corollary 5. *For \mathbf{w} in Corollary 4, there exists differentiable functions \mathbf{m} and σ such that $\mathbf{f}(\mathbf{x}) = S(\mathbf{x})^{-1}U\mathbf{w}(\mathbf{x})$ is not differentiable globally on \mathbb{R}^n .*

Proof. For the counter example, let $\mathbf{m} : \mathbb{R}^3 \rightarrow \mathbb{R}^3$ be a constant function $\mathbf{m}(\mathbf{x}) = [1, 1, 1]^\top$, and $\sigma(a) = a^2$. It is easy to verify that they both satisfy the conditions in Corollary 4 and are differentiable. We show that the partial derivative $\frac{\partial \mathbf{f}_1(\mathbf{x})}{\partial \mathbf{x}_3}$ does not exists at $\mathbf{x} = [2, 1, 1]^\top$. With few simple steps one could see $\mathbf{f}_1(\mathbf{x} + \alpha \mathbf{e}_3)$ for $\alpha \in (-\infty, 1]$ is

$$\mathbf{f}_1(\mathbf{x} + \alpha \mathbf{e}_3) = \begin{cases} \sigma(1) + \sigma(-\alpha) + 1 & \alpha \leq 0 \\ \sigma(1 - \alpha) + \sigma(\alpha) + 1 & 0 < \alpha \leq 1 \end{cases} \quad (6)$$

Though this function is continuous, the left and right derivatives are not equal at $\alpha = 0$ so the function is not differentiable at $\mathbf{x} = [2, 1, 1]^\top$. ■

The above example shows that \mathbf{f} may not be differentiable for tied inputs. On the other hand, it is straightforward to see function \mathbf{f} is differentiable at points where there is no tie. More precisely, for the points with tie in the input vector, we show the function \mathbf{f} is B-differentiable, which is a weaker condition than the usual (Frechét) differentiability.

Definition 7. (Facchinei & Pang, 2007) A function $\mathbf{f} : \mathbb{R}^n \rightarrow \mathbb{R}^m$ is said to be *B(ouligand)-differentiable* at a point $\mathbf{x} \in \mathbb{R}^n$, if \mathbf{f} is Lipschitz continuous in the neighborhood of \mathbf{x} and directionally differentiable at \mathbf{x} .

Proposition 3. For $\mathbf{f} : \mathbb{R}^n \rightarrow \mathbb{R}^n$ in Theorem 1, let $\mathbf{w}(\mathbf{x})$ be as defined in Corollary 4. If σ and \mathbf{m} are continuously differentiable, then \mathbf{f} is B-differentiable on \mathbb{R}^n .

Proof. Let $\mathbb{P}^n = \{P_1, \dots, P_K\}$ be the finite set of all possible $n \times n$ dimensional permutation matrices. For each $k \in [K]$, define the closed set $\mathbb{N}_k = \{\mathbf{x} : S(\mathbf{x})\mathbf{x} = P_k\mathbf{x}\}$. These sets are convex polyhedrons since each can be defined by a finite set of linear inequalities; in addition, they together form a covering set of \mathbb{R}^n .

If there is no tie in elements of vector \mathbf{x} , then $\mathbf{x} \in \text{int}(\mathbb{N}_k)$ for some $k \in [K]$. Since the sorting function $S(\mathbf{x})$ has the constant value P_k in a small enough neighborhood of \mathbf{x} , the function \mathbf{f} is continuously differentiable (and therefore B-differentiable) at \mathbf{x} .

Next we show that, for any point $\mathbf{x} \in \mathbb{R}^n$ with some tied elements, the directional derivative of \mathbf{f} along an arbitrary direction $\mathbf{d} \in \mathbb{R}^n$ exists. For such \mathbf{x} and \mathbf{d} , there exists a $k \in [K]$ and a small enough $\delta > 0$ such that $\mathbf{x}, \mathbf{x} + \epsilon\mathbf{d} \in \mathbb{N}_k$ for all $0 \leq \epsilon \leq \delta$. Therefore, we have $\mathbf{f}(\mathbf{x}') = \hat{\mathbf{f}}(\mathbf{x}')$ for all $\mathbf{x}' \in [\mathbf{x}, \mathbf{x} + \delta\mathbf{d}]$, where $\hat{\mathbf{f}}_k(\mathbf{x}) = P_k^{-1}UD(P_k\mathbf{x})\mathbf{m}(\mathbf{x})$. Let $\hat{\mathbf{f}}'_k(\mathbf{x}; \mathbf{d})$ denote the directional derivative of $\hat{\mathbf{f}}_k$ at \mathbf{x} along \mathbf{d} . By the equality of $\hat{\mathbf{f}}_k$ and \mathbf{f} in $[\mathbf{x}, \mathbf{x} + \delta\mathbf{d}]$, we conclude that the directional derivative $\mathbf{f}'(\mathbf{x}; \mathbf{d})$ exists and is equal to $\hat{\mathbf{f}}'_k(\mathbf{x}; \mathbf{d})$.

Finally, we note that \mathbf{f} is Lipschitz continuous, since it is composed by pieces of Lipschitz continuous functions $\hat{\mathbf{f}}_k$ for $k \in [K]$ (implied by the continuous differentiability assumption on σ and \mathbf{m}). Thus, \mathbf{f} is B-differentiable. ■

C. Reliability Diagrams

Fig. 5 illustrates the reliability diagram for different calibration algorithms in ResNet 152 and DenseNet 161 models on ImageNet dataset. The DIAGONAL method outperforms other methods in calibration in most of the regions. OP and OI methods also achieve good calibration performance on this dataset and are slightly better than temperature scaling, while MS-ODIR and Dir-ODIR methods do not reduce the calibration error as much on this dataset.

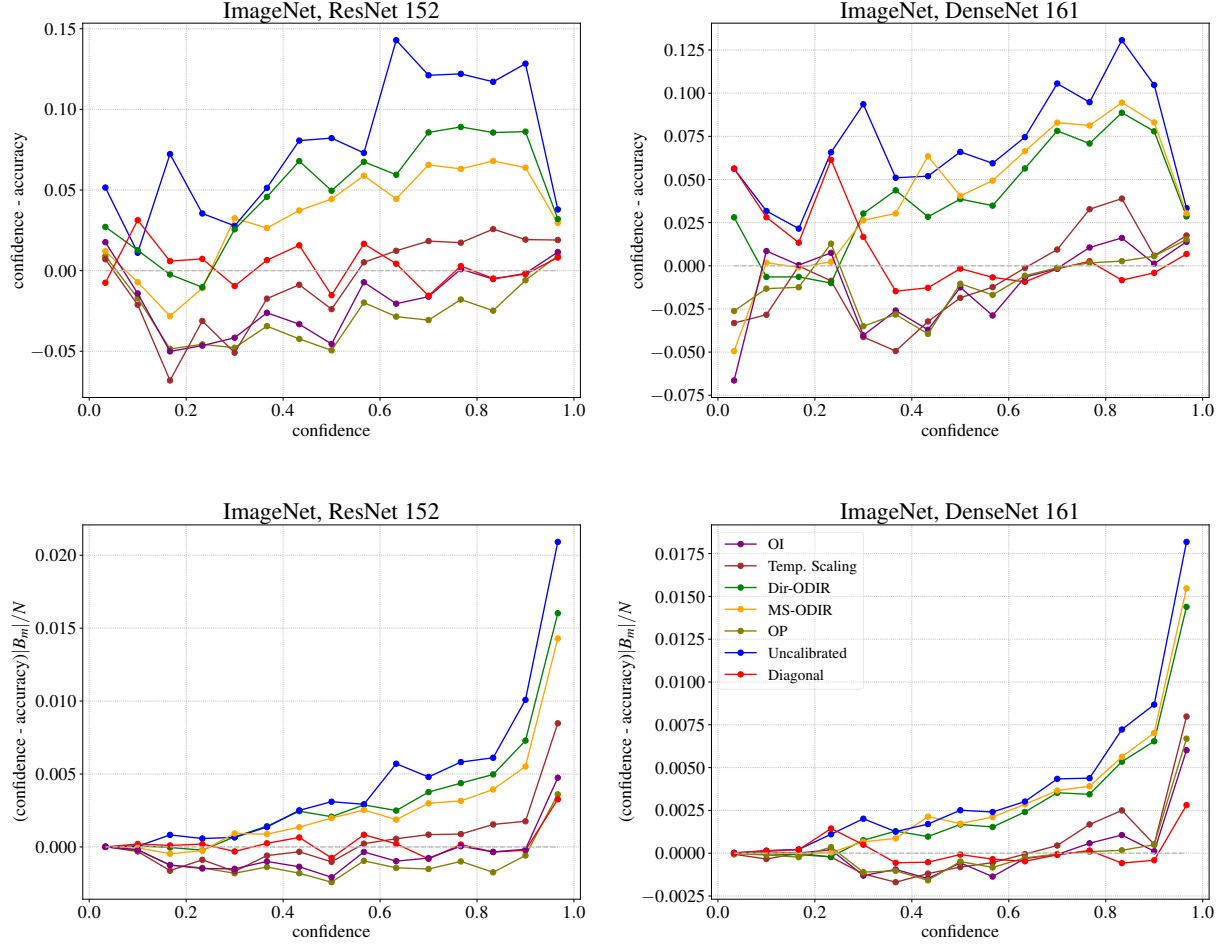


Figure 5. Reliability diagrams for ResNet 152 and DenseNet 161 on ImageNet. Confidence is the maximum softmax output of the corresponding network. As suggested by (Maddox et al., 2019) we show the difference between the estimated confidence and accuracy (instead of showing the confidence and accuracy plot separately) over $M = 15$ bins in the top row. In the bottom row the different is weighted by frequency of data in each bin. The dashed grey lines represent the perfectly calibrated network. Points above (below) the grey line shows overconfident (underconfident) predictions in a bin. Since the uncalibrated network has different distances to the perfect calibration in different regions, scaling by a single temperature will lead to a mix of underconfident and overconfident regions. The DIAGONAL function, on the other hand, has more flexibility to reduce the calibration error.